Lab Rotation Report

Peter Waldert

29^{th} of February, 2024

1 Summary

2 Introduction

This lab rotation was concerned with the development, exploration and implementation of a new optimisation approach for the reconstruction of current density / conductivity of tissue within a Magnetic Resonance Imaging (MRI) setup.

The overall intention of MRI is to turn a source of contrast into an image for clinicians to use, mainly for the identification of different (potentially malignant) tissue types. In the usual setting, this source of contrast is one of T_1, T_2 or T_2^*, three material constants. Visualising these material properties in an image therefore allows to differentiate between different types of tissue visually.

2.1 Mathematical Introduction to Magnetic Resonance Imaging

The general equation governing the behaviour of these *spin* objects is the Bloch equation:

$$\frac{\mathrm{d}\boldsymbol{M}}{\mathrm{d}t} = \gamma(\boldsymbol{M} \times \boldsymbol{B})\,. \tag{1}$$

2.2 The Biot-Savart Law

For a given current density $\boldsymbol{j}(t) : \Omega \to \mathbb{R}^3$ [1] on a domain $\Omega \subseteq \mathbb{R}^3$ at time $t \in \mathbb{R}^+$, Maxwell's fourth equation in differential form

$$\nabla \times \boldsymbol{B} = \mu_0 \left(\boldsymbol{j} + \varepsilon_0 \frac{\partial \boldsymbol{E}}{\partial t} \right)\,,$$

relates the curl of the magnetic field $\boldsymbol{B}(t) : \Omega \to \mathbb{R}^3$ to the current density $\boldsymbol{j}(t)$ and the temporal rate of change in the *electric* field $\boldsymbol{E}(t) : \Omega \to \mathbb{R}^3$. ε_0 and μ_0 are the electric permittivity and magnetic permeability of free space, respectively. The current density $\boldsymbol{j}$ is also connected to the electric field $\boldsymbol{E}$ through the, also position-dependent, electrical conductivity $\sigma : \Omega \to \mathbb{R}^+$

$$\boldsymbol{j} = \sigma \boldsymbol{E}\,.$$

[1] The current density $\boldsymbol{j} = nq\boldsymbol{v}$, describing the flow of n charges q with velocity $\boldsymbol{v}$, may be related to *current* I through the infinitesimal $\boldsymbol{j}\,\mathrm{d}^3\boldsymbol{x} = I\,\mathrm{d}\boldsymbol{x}$.

In the **electrostatic case** (when the electric field $\boldsymbol{E}$ is indepent of time t), the last term in the above equation will vanish and we arrive at

$$\nabla \times \boldsymbol{B} = \mu_0 \boldsymbol{j}\,.$$

This equation, together with the freedom of divergence of the magnetic field (Maxwell's second equation), $\nabla \cdot \boldsymbol{B} = 0$, leads to the **Biot-Savart law**

$$\boldsymbol{B}(\boldsymbol{x}) = \frac{\mu_0}{4\pi}\int_\Omega \frac{\boldsymbol{j}(\boldsymbol{y}) \times (\boldsymbol{x}-\boldsymbol{y})}{\|\boldsymbol{x}-\boldsymbol{y}\|_2^3}\,\mathrm{d}\boldsymbol{y} = \frac{\mu_0}{4\pi}\int_\Omega \frac{\boldsymbol{j}(\boldsymbol{y}) \times \boldsymbol{y}}{\|\boldsymbol{y}\|_2^3}\,\mathrm{d}\boldsymbol{y} \tag{2}$$

which provides an explicit expression for the magnetic field contribution $\boldsymbol{B}(\boldsymbol{x})$ at position $\boldsymbol{x} \in \Omega$ given a current density field $\boldsymbol{j}$.

2.3 Current Density Imaging

3 Methods

For visualisation and as a general framework, we built upon the **KomaMRI** toolchain and Julia software package (Castillo-Passi et al. 2022). This choice made sense because of its feature-richness and further extensibility.

3.1 Gridded Data Format

In order to use KomaMRI together with the Fast Fourier Transform (FFT)-based, we had to adapt the storage format.

3.2 FFT-accelerated evaluation of the Biot-Savart law

Starting from the Biot-Savart law introduced above (cf. Equation (2)), we observe that splitting the cross-product ($\times$) into its three respective components

$$\begin{aligned}
B_1(\boldsymbol{x}) &= \frac{\mu_0}{4\pi}\int_\Omega \frac{j_2(\boldsymbol{y})\cdot(\boldsymbol{x}_3-\boldsymbol{y}_3) - j_3(\boldsymbol{y})\cdot(\boldsymbol{x}_2-\boldsymbol{y}_2)}{\|\boldsymbol{x}-\boldsymbol{y}\|_2^3}\,\mathrm{d}\boldsymbol{y}\,,\\
B_2(\boldsymbol{x}) &= \frac{\mu_0}{4\pi}\int_\Omega \frac{j_3(\boldsymbol{y})\cdot(\boldsymbol{x}_1-\boldsymbol{y}_1) - j_1(\boldsymbol{y})\cdot(\boldsymbol{x}_3-\boldsymbol{y}_3)}{\|\boldsymbol{x}-\boldsymbol{y}\|_2^3}\,\mathrm{d}\boldsymbol{y}\,,\\
B_3(\boldsymbol{x}) &= \frac{\mu_0}{4\pi}\int_\Omega \frac{j_1(\boldsymbol{y})\cdot(\boldsymbol{x}_2-\boldsymbol{y}_2) - j_2(\boldsymbol{y})\cdot(\boldsymbol{x}_1-\boldsymbol{y}_1)}{\|\boldsymbol{x}-\boldsymbol{y}\|_2^3}\,\mathrm{d}\boldsymbol{y}\,,
\end{aligned}$$

according to the explicit representation of the cross-product $\times$ in three spatial dimensions, most notably allows us to express B_1, B_2 and B_3 as convolution integrals

$$B_1(\boldsymbol{x}) = \frac{\mu_0}{4\pi}\int_\Omega \Big[j_2(\boldsymbol{y})g_3(\boldsymbol{x}-\boldsymbol{y}) - j_3(\boldsymbol{y})g_2(\boldsymbol{x}-\boldsymbol{y})\Big]\,\mathrm{d}\boldsymbol{y} = \frac{\mu_0}{4\pi}\Big[(j_2 *_\Omega g_3) - (j_3 *_\Omega g_2)\Big](\boldsymbol{x})\,,$$

with $g_1, g_2, g_3 : \Omega \to \mathbb{R}$, $g_1(\boldsymbol{x}) = \frac{\boldsymbol{x}_1}{\|\boldsymbol{x}\|_2^3}$, $g_2(\boldsymbol{x}) = \frac{\boldsymbol{x}_2}{\|\boldsymbol{x}\|_2^3}$ and $g_3(\boldsymbol{x}) = \frac{\boldsymbol{x}_3}{\|\boldsymbol{x}\|_2^3}$ and the respective analogs for B_2 and B_3 (Yazdanian et al. 2020).

Using the convolution theorem

$$\mathcal{F}[f * g](\boldsymbol{k}) = \mathcal{F}[f](\boldsymbol{k}) \cdot \mathcal{F}[g](\boldsymbol{k}) \quad \text{where} \quad \mathcal{F}[f](\boldsymbol{k}) := \int f(\boldsymbol{x})\mathrm{e}^{-\mathrm{i}\boldsymbol{k}\boldsymbol{x}}\,\mathrm{d}\boldsymbol{x}\,,$$

(for more information, we refer the reader to Herman 2022), the respective convolution integrals may be evaluated "much faster" using the FFT and IFFT. More precisely, this speedup is due to the computational complexity cost reduction from $\mathcal{O}(n^2)$ to $\mathcal{O}(n \log n)$.

The first component of the magnetic field $B_1 = \{\boldsymbol{B}\}_1$ may then be expressed as

$$B_1(\boldsymbol{x}) = \frac{\mu_0}{4\pi} \mathcal{F}^{-1} \left[\mathcal{F}(j_2) \cdot \mathcal{F}(g_3) - \mathcal{F}(j_3) \cdot \mathcal{F}(g_2) \right] (\boldsymbol{x}) \,,$$

and analogous expressions may be found for the second and third component B_2 and B_3, respectively. Importantly, we can explicitly evaluate

$$\mathcal{F}[g_n](\boldsymbol{k}) = \mathcal{F} \left[\boldsymbol{x} \mapsto \frac{x_n}{\|\boldsymbol{x}\|_2^3} \right] (\boldsymbol{k}) = -\mathrm{i} \frac{k_n}{\|\boldsymbol{k}\|_2^2} \,, \quad \text{for } n = 1, 2, 3 \,,$$

which allows for a direct evaluation of the above using only the FFT, IFFT, addition and multiplication (Yazdanian et al. 2020).

In code, this may be implemented like so:

```
cross(a1, a2, a3, b1, b2, b3) = (
  a2 .* b3 - a3 .* b2,
  -(a1 .* b3 - a3 .* b1),
  a1 .* b2 - a2 .* b1
)

function calculate_magnetic_field(cdp::CurrentDensityPhantom)::VectorField
  # [obtain M_range, calculate g1, g2, g3 on the entire frequency domain]
  c1, c2, c3 = cross(fft(pad_jx), fft(pad_jy), fft(pad_jz), g1, g2, g3)
  B1, B2, B3 = real(ifft(c1)), real(ifft(c2)), real(ifft(c3))
  return mu_0 .* (B1[M_range...], B2[M_range...], B3[M_range...])
end
```

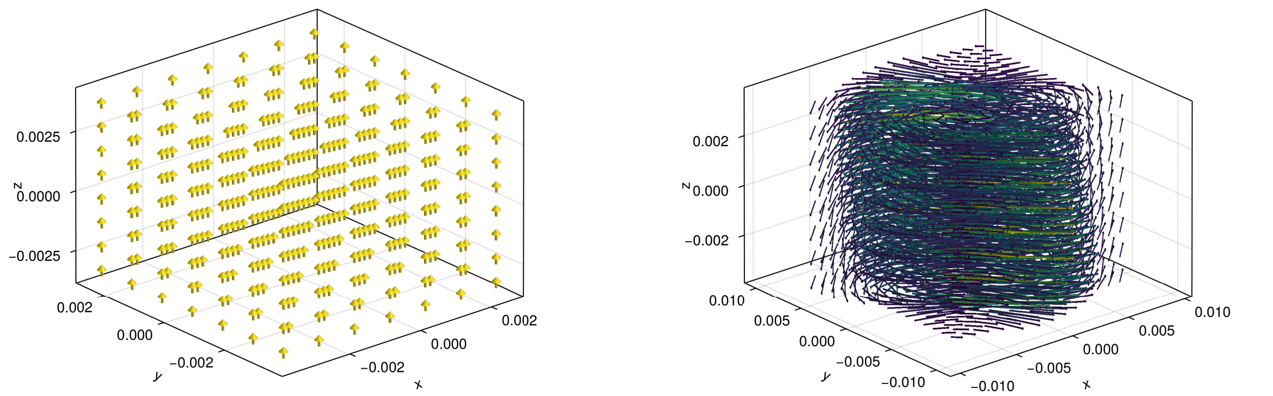

(a) Exemplary uniform, homogeneous current density vector field $\boldsymbol{j}(\boldsymbol{x}) = j_0 \hat{\boldsymbol{e}}_z \mathbb{1}_{\boldsymbol{x} \in \Omega_s}$ on a sample rectangular domain.

(b) Magnetic field $\boldsymbol{B}(\boldsymbol{x})$ resulting from the homogeneous current density field depicted in Figure 1a.

4 Results

5 Future Perspectives

5.1 Usage as a Julia Package

References

Castillo-Passi, Carlos, Ronal Coronado, Gabriel Varela-Mattatall, Carlos Alberola-López, René Botnar and Pablo Irarrazaval (2022). 'KomaMRI.jl: An open-source framework for general MRI simulations with GPU acceleration'. In: *Magnetic Resonance in Medicine*. DOI: 10.1002/mrm.29635. eprint: https://onlinelibrary.wiley.com/doi/pdf/10.1002/mrm.29635.

Yazdanian, Hassan, Guilherme B. Saturnino, Axel Thielscher and Kim Knudsen (June 2020). 'Fast evaluation of the Biot-Savart integral using FFT for electrical conductivity imaging'. In: *J. Comput. Phys.* 411, p. 109408. ISSN: 0021-9991. DOI: 10.1016/j.jcp.2020.109408.

Herman, Russell (July 2022). '9.9: The Convolution Theorem'. In: *Mathematics LibreTexts*. URL: https://math.libretexts.org/Bookshelves/Differential_Equations/Introduction_to_Partial_Differential_Equations_(Herman)/09%3A_Transform_Techniques_in_Physics/9.09%3A_The_Convolution_Theorem.

Acronyms

FFT	Fast Fourier Transform	2
IFFT	Inverse Fast Fourier Transform	3
MRI	Magnetic Resonance Imaging	1